V.I.1 Performance of Advanced Automotive Fuel Cell Systems with Heat Rejection Constraints

Rajesh K. Ahluwalia (Primary Contact),
Xiaohua Wang
Argonne National Laboratory
9700 South Cass Avenue
Argonne, IL 60439
Phone: (630) 252-5979
Email: walia@anl.gov

DOE Manager
Nancy Garland
Phone: (202) 586-5673
Email: Nancy.Garland@ee.doe.gov

Project Start Date: October 1, 2003
Project End Date: Project continuation and direction determined annually by DOE

Overall Objectives

- Develop a validated model for automotive fuel cell systems, and use it to assess the status of the technology.
- Conduct studies to improve performance and packaging, to reduce cost, and to identify key R&D issues.
- Compare and assess alternative configurations and systems for transportation and stationary applications.
- Support DOE/U.S. Driving Research and Innovation for Vehicle efficiency and Energy sustainability (U.S. DRIVE) automotive fuel cell development efforts.

Fiscal Year (FY) 2014 Objectives

- Further develop and validate the stack model for membrane electrode assemblies (MEAs) with 3M's nanostructured thin-film (NSTF) catalysts for applicability to hotter and drier operating conditions.
- Develop a methodology to analyze the performance of automotive fuel cells subject to the recently imposed heat rejection constraint ($Q/\Delta T = 1.45$ kW/°C).
- Determine the optimum operating conditions for minimum system cost subject to the $Q/\Delta T$ constraint.
- Provide component specifications and operating conditions to the detailed fuel cell system cost study.

Technical Barriers

This project addresses the following technical barriers from the Fuel Cells section of the Fuel Cell Technologies Office Multi-Year Research, Development, and Demonstration Plan:

(B) Cost

(C) Performance

Technical Targets

This project is conducting system-level analyses to address the following DOE 2020 technical targets for automotive fuel cell power systems operating on direct hydrogen:

- Energy efficiency: 60% at 25% of rated power
- $Q/\Delta T$: 1.45 kW/°C
- Power density: 650 W/L for system, 2,500 W/L for stack
- Specific power: 650 W/kg for system, 2,000 W/kg for stack
- Transient response: 1 s from 10% to 90% of rated power
- Start-up time: 30 s from –20°C and 5 s from +20°C ambient temperature
- Precious metal content: 0.125 g/kW

FY 2014 Accomplishments

- Collaborated with 3M in taking cell data to validate the model for NSTF catalyst-based MEAs and stacks.
- Developed a correlation for limiting current densities for MEAs with PtCoMn/NSTF catalyst.
- Developed a rational model for mass transfer overpotentials in PtCoMn/NSTF cathode catalyst.
- Validated the cell model over a wide range of operating pressures, temperatures, relative humidities, and stoichiometries.
- Conducted a comprehensive study to investigate the impact of the heat rejection constraint ($Q/\Delta T$) on fuel cell system operation, performance, and cost.

✧ ✧ ✧ ✧ ✧

INTRODUCTION

While different developers are addressing improvements in individual components and subsystems in automotive fuel cell propulsion systems (i.e., cells, stacks, balance-of-plant components), we are using modeling and analysis to address issues of thermal and water management, design-point and part-load operation, and component-, system-, and vehicle-level efficiency and fuel economy. Such analyses are essential for effective system integration.

APPROACH

Two sets of models are being developed. The GCtool software is a stand-alone code with capabilities for design, off-design, steady-state, transient, and constrained optimization analyses of fuel cell systems. A companion code, GCtool-ENG, has an alternative set of models with a built-in procedure for translation to the MATLAB®/Simulink® platform commonly used in vehicle simulation codes, such as Autonomie.

RESULTS

In FY 2014, we continued to collaborate with 3M to obtain reference performance data on 50-cm^2 active-area single cells using MEAs that consisted of 3M 24-µm membrane (850 equivalent weight), ternary $Pt_{0.68}Co_{0.3}Mn_{0.02}$/NSTF catalyst, and 3M gas diffusion layers made by applying a hydrophobic treatment to a backing paper and a micro-porous layer [1]. The Pt loading was 0.050 mg·cm^{-2} in the anode and 0.054, 0.103, 0.146 or 0.186 mg·cm^{-2} in the cathode.

For applicability to hotter and drier conditions, we reanalyzed the available polarization data to develop a rational model for mass transfer overpotentials in ternary PtCoMn/NSTF catalysts. The approach was to first define a limiting current density (i_L) at which the mass transfer overpotential equals a set value of 0.45 V. This limiting current density was determined from the cell polarization data and was correlated as a function of the operating pressure (P), temperature (T), oxygen mole fraction (X_{O2}), relative humidity (RH) and gas velocity in flow channel. Figure 1a compares the i_L correlation with the experimental data for tests at different pressures and temperatures and 100% RH at cell exit. The accuracy of the correlation could be improved if the experimental data were obtained in differential cells or if the tests were run at high stoichiometries with one variable changing at a time.

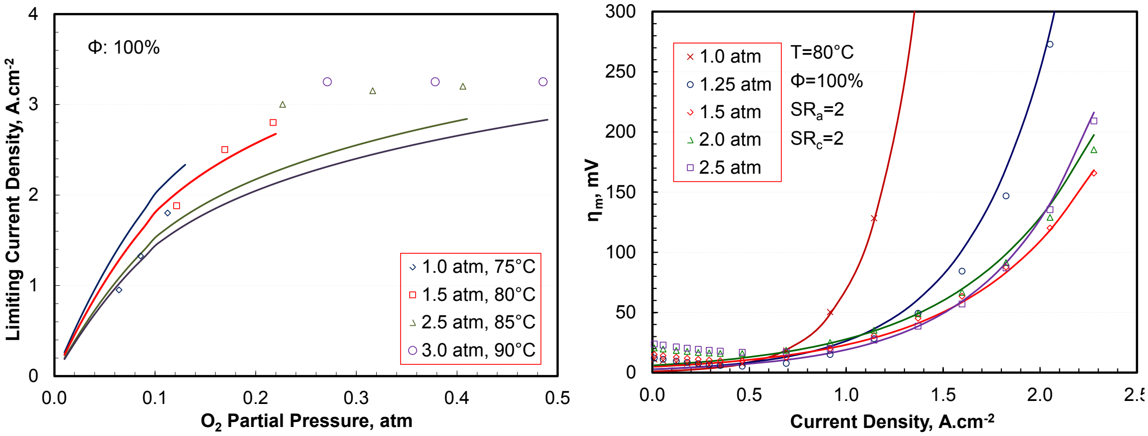

(a) Limiting current density correlation (b) Mass transfer overpotential correlation

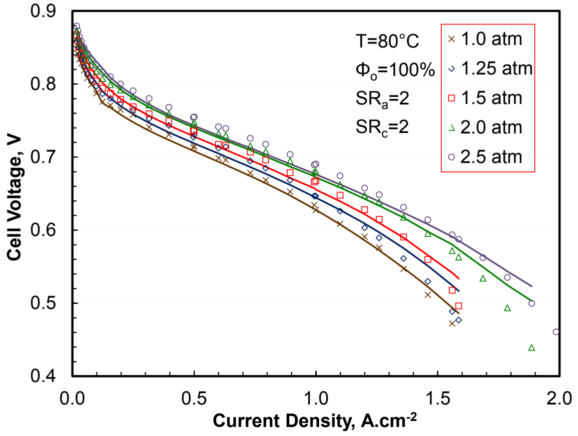

(c) Validation of the cell model

FIGURE 1. Development and validation of the cell performance model. The data are shown for 100% RH (Φ) and a cell with 3M MEA and ternary PtCoMn/NSTF catalysts. Pt loading is 0.104 mg_{Pt}·cm^{-2} in the cathode and 0.05 mg_{Pt}·cm^{-2} in the anode.

The second step was to correlate the mass transfer overpotential (η_m) in terms of the reduced current density (i/i_L), i.e., the current density (i) normalized by i_L. Second order terms were included in the η_m correlation to correct for P, T, X_{O2}, RH, and gas velocity. Figure 1b compares the correlation with the experimental data for one series of tests in which the exit pressure was changed from 1 atm to 2.5 atm. The comparison is equally good for other series of tests with T, RH, and anode/cathode stoichiometric ratio (SR) as variables.

The rational model for η_m was incorporated in the multi-nodal cell model that also has modules for calculating the activation overpotentials for the oxygen reduction reaction on cathode [1] and hydrogen oxidation reaction on anode [2]; anode mass transfer overpotentials because of nitrogen buildup; and ohmic overpotentials in the membrane, gas diffusion layer, and membrane/gas diffusion layer interface. Figure 1c compares the model results with the experimental polarization curves for the pressure series of tests as in Figure 1b. The comparison is equally good for other series of tests with T, RH, and anode/cathode SR as variables.

System Performance

The updated cell model was used to analyze the performance of an 80-kW_{net} fuel cell system (see Refs. [3,4] for system configuration) with ternary PtCoMn/NSTF catalysts in the polymer electrolyte fuel cell (PEFC) stack. Table 1 lists the important parameters of the components comprising the stack, fuel management system, air management system, heat rejection system, and water management system. An optimization study was conducted to determine the coolant exit temperature (limited to 95°C), dew point temperature of cathode air at stack inlet, and cell voltage for minimum system cost, subject to the $Q/\Delta T$ constraint of 1.45 kW/°C, for specified Pt loading in anode and cathode catalysts. Here Q is the stack heat load and ΔT is the difference between the coolant stack outlet temperature and the ambient (heat sink) temperature taken as 40°C. For comparison with previous results, the study was repeated for 100% stack exit RH.

The physical coupling of the PEFC stack and the upstream membrane humidifier determines the approach dew point temperature at cathode inlet and establishes the relationship between the optimum stack coolant exit temperature (T_c) and cathode stoichiometric ratio (SR_c) as a function of the stack operating pressure. For 100% stack exit RH, T_c is limited to 82°C at 1.5 atm, 87°C at 2 atm, 92°C at 2.5 atm, and 95°C at 3 atm, if SR_c is held at 1.5; T_c is lower, especially at low operating pressures (8°C lower at 1.5 atm), if SR_c is raised to 2.5. Without any restriction on stack exit RH, T_c increases to 90°C at 1.5 atm for a SR_c of 1.5.

Figure 2 shows the cell voltage and the corresponding system efficiency needed at rated power to satisfy the $Q/\Delta T$ constraint. The results indicate that low stack inlet pressures (1.5 atm) with 100% exit RH may not be acceptable because the coolant exit temperature is restricted to <82°C, ΔT to <42°C, and Q to <61 kW, so that the required cell voltage has to be >740 mV. The required cell voltage at 1.5 atm stack inlet pressure is 65 mV lower if the stack is operated hotter (90°C vs. 82°C) and drier (83% RH vs. 100% RH). Over the range of SR_c investigated, 1.5–2.5, the required cell voltage is lowest at SR_c of 1.5.

TABLE 1. Critical Parameters for Various Components of the Fuel Cell System

PEFC Stack

- 1.5 -3 atm at rated power
- 40 -67% O_2 utilization (SR_c: 1.5 -2.5)
- 50% H_2 consumption per pass
- Cell voltage at rated power: TBD
- 24 -μm 3M membrane at TBD temperature
- 3M ternary alloy: 0.1/0.05 mg -Pt/cm^2 on cathode/anode
- GDL: 235 -μm non - woven carbon fiber with MPL
- 1.1 -mm metal bipolar plates, each with cooling channels
- 17 cells/inch

Fuel Management System

- Hybrid ejector - recirculation pump
- 35% pump efficiency
- 3 psi pressure drop at rated power

Air Management System

- Compressor -expander module
- Liquid -cooled motor
- Efficiencies at rated power: 71% compressor, 73% expander, 89.5% motor, 89.5% controller
- Turn -down: 20
- 5 psi pressure drop at rated power

Heat Rejection System

- Two circuits: 75 -95 °C HT, 10 °C ΔT
  65 °C LT coolant, 5° C ΔT
- 55% pump + 92% motor efficiency
- 45% blower + 92% motor efficiency
- 10 psi pressure drop in the stack and 5 psi pressure drop in the radiator

Water Management System

- Membrane humidifier, TBD dew -point temperature at rated power

TBD – to be determined; GDL – gas diffusion layer; LT – low temperature ; MPL - microporous layer; HT - high temperature

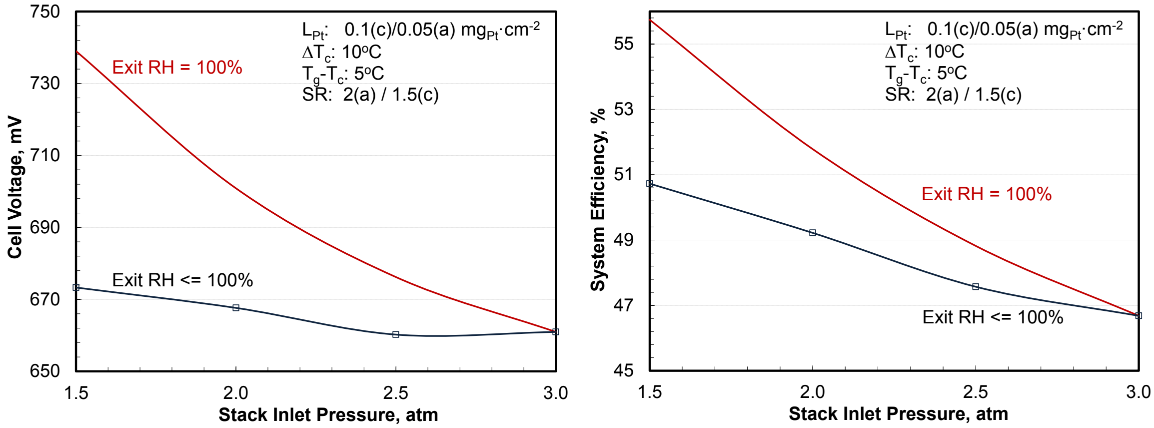

(a) Cell voltage (b) System efficiency

FIGURE 2. Cell Voltage and the Corresponding System Efficiency Needed to meet the Q/ΔT Constraint at Different Stack Inlet Pressures

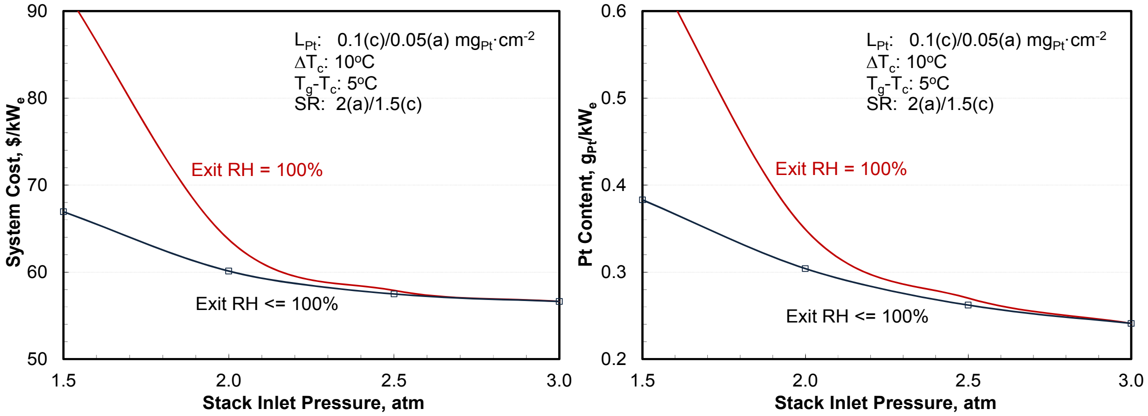

(a) System cost (b) Platinum content

FIGURE 3. Results of an optimization study for minimum system cost subject to Q/ΔT constraint. The various symbols in the legend are for anode (a) and cathode (c) Pt loadings (L_{Pt}), coolant temperature rise in stack (ΔT_c), difference in MEA and coolant temperatures (T_g-T_c) and anode and cathode SRs.

Figure 2a indicates that, for 100% exit RH and SR_c of 1.5, the required cell voltage decreases sharply as the stack inlet pressure is raised from 1.5 atm to 3 atm. This decrease in required cell voltage is slower if the cathode exit RH is optimized and not restricted to 100%. The stack power density is <500 $mW{\cdot}cm^{-2}$ for stack operating pressures below 1.8 to 2 atm. The difference in power densities for restricted (100%) and unrestricted (<100%) RH diminishes as the stack inlet pressure is raised above 2.5 atm since, even without the RH restriction, the optimum cathode exit RH approaches 100%.

Figure 2b presents the power conversion efficiency (lower heating value basis) that the fuel cell system must have in order to meet the Q/ΔT constraint at rated power. Imposing the heat rejection constraint makes the system efficiency at rated power a function of the operating pressure. The required efficiency is lower (desired result) at higher stack inlet pressures or if the cathode exit RH is less than 100% (although there are durability implications). Note that the anode outlet may contain condensed water; the stack heat load includes this latent heat and the sensible heat loads due to rise in gas temperatures in addition to the waste heat generated (related to cell voltage) by the thermodynamic irreversibilities in the cell electrochemical reactions (i.e., cell overpotentials).

Figure 3 presents the system cost ($\$/kW_e$) and Pt content ($g/kW_e$) under optimum operating conditions. The system cost in this study has been estimated using correlations provided by Strategic Analysis, Inc. for high-volume manufacturing (500,000 units/year) and a Pt price of $1,500/tr-oz [5]. Consistent with the results in Figure 2a, the differences in system cost and Pt content between saturated (RH = 100%) and superheated (RH < 100%) cathode exits are large at low operating pressures and diminish at higher

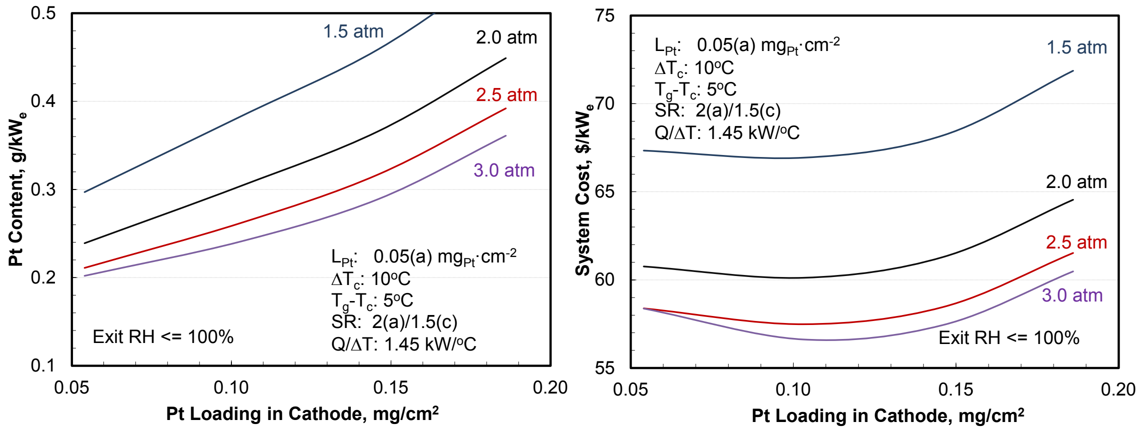

(a) Platinum content (b) System cost

FIGURE 4. Pt Content and System Cost as Function of Pt Loading in Cathode Catalyst, 2.5-atm Stack Inlet Pressure

operating pressures. The lowest system cost is at 3-atm stack inlet pressure, although the cost saving is small compared to 2.5-atm stack inlet pressure. The optimum cathode exit RH is >95% if the stack inlet pressure is higher than 2.5 atm, and it is <83% if the inlet pressure is 1.5 atm.

A parametric study was conducted to determine the optimum Pt loading in the cathode catalyst for 2.5-atm stack inlet pressure. Figure 4a shows that the cathode with the smallest Pt loading considered in this study (0.054 $mg_{Pt}\cdot cm^{-2}$) has the lowest Pt content but also the lowest power density (see Table 2). The system cost is lowest for cathode Pt loading between 0.1 and 0.125 $mg\cdot cm^{-2}$, although the power density is highest for 0.146 $mg\cdot cm^{-2}$ Pt loading (see Table 2). The optimum Pt loading in cathode would be higher if the Pt price was $1,100/tr-oz rather than $1,500/tr-oz assumed in this study.

TABLE 2. Effect of Cathode Pt Loading on Stack Performance and Cost

Pt Loading	mg/cm^2	0.054	0.103	0.146	0.186
Power Density	mW/cm^2	541	641	679	660
Pt Cost	$/kW$_e$	10.2	12.6	15.3	18.9
Stack Cost	$/kW$_e$	28.8	29.2	31.1	35.1

CONCLUSIONS AND FUTURE DIRECTIONS

- Meeting the Q/ΔT constraint requires that the stack be operated hotter (coolant exit temperature >90°C), drier (stack exit RH <100%), and at elevated pressures (inlet pressures >2 atm).
- Under optimum conditions, the projected Pt content and cost of an 80-kWe fuel cell system that meets the 1.45 kW/°C constraint are 0.27 g/kW$_e$ and 57.9 $/kW$_e$. The stack in this system has ternary PtCoMn/NSTF catalysts with Pt loading of 0.104 $mg\cdot cm^{-2}$ in the cathode and 0.05 $mg\cdot cm^{-2}$ in the anode.
- Stack durability under operating conditions needed to meet the heat rejection requirement is a concern. In FY 2015, we will develop a model to investigate the durability of NSTF MEAs under an automotive duty cycle that includes heat rejection at peak power.
- In FY 2015, we will continue to evaluate alternative advanced catalysts on NSTF and corrosion-resistant carbon supports. We will also continue our collaboration with Eaton on developing and modeling a Roots air management system.

FY 2014 PUBLICATIONS/PRESENTATIONS

1. R.K. Ahluwalia, S. Arisetty, J-K Peng, R. Subbaraman, X. Wang, N. Kariuki, D.J. Myers, R. Mukundan, R. Borup, and O. Polevaya, “Dynamics of Particle Growth and Electrochemical Surface Area Loss due to Platinum Dissolution,” Journal of the Electrochemical Society, 161 (3) F291-F304 (2013).

2. S. Ahmed, D.P. Papadias, and R.K. Ahluwalia, “Configuring a Fuel Cell based Residential Combined Heat and Power System,” Journal of Power Sources, 242, 884-894 (2013).

3. D.D. Papadias, R.K. Ahluwalia, J.K. Thomson, H.M. Meyer III, M.P. Brady, H. Wang, R. Mukundan, and R. Borup, “Degradation of SS316L Bipolar Plates in Fuel Cell Environment: Corrosion Rate, Barrier Film Formation Kinetics and Contact Resistance,” accepted for publication in Journal of Power Sources, (2014).

4. T.Q. Hua, R.K. Ahluwalia, L. Eudy, G. Singer, B. Jermer, N. Asselin-Miller and T. Patterson, “Status of Hydrogen Fuel Cell Electric Buses Worldwide,” submitted to Journal of Power Sources, (2014).

5. N. Garland and R.K. Ahluwalia, “Report from the Annexes: Annex 26,” IEA AFC ExCo 46th Meeting, Salzburg, Austria, May 22-23, 2013.

REFERENCES

1. R.K. Ahluwalia, X. Wang, A. Lajunen, A.J. Steinbach, S.M. Hendricks, M.J. Kurkowski, and M.K. Debe, "Kinetics of Oxygen Reduction Reaction on Nanostructured Thin-Film Platinum Alloy Catalyst," J. Power Sources, 215, 77-88, 2012.

2. X. Wang, R.K. Ahluwalia, and A.J. Steinbach, "Kinetics of Hydrogen Oxidation and Hydrogen Evolution Reactions on Nanostructured Thin-Film Platinum Alloy Catalyst," J. Electrochemical Society, 160 (3) F251-F261, 2013.

3. R.K. Ahluwalia, X. Wang, J. Kwon, and A. Rousseau, "Drive-Cycle Performance and Life-Cycle Costs of Automotive Fuel Cell Systems," 2011 Fuel Cell Seminar & Exposition, Orlando, FL, October 31 – November 2, 2011.

4. R.K. Ahluwalia, X. Wang, J. Kwon, A. Rousseau, J. Kalinoski, B. James, and J. Marcinkoski, "Performance and Cost of Automotive Fuel Cell Systems with Ultra-Low Platinum Loadings," J. Power Sources, 196, 4619, 2011.

5. B.D. James, J.A. Kalinoski, and K.N. Baum, "Mass Production Cost Estimation for Direct H_2 PEM Fuel Cell Systems for Automotive Applications: 2009 Update," DTI Report GS-10F-0099J, January 2010.